Published in the Slovak Republic
European Reviews of Chemical Research
Has been issued since 2014.
E-ISSN: 2413-7243
2019, 6(1): 12-22

DOI: 10.13187/ercr.2019.1.12
www.ejournal14.com

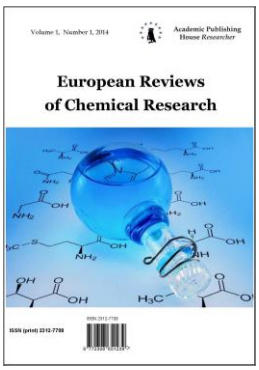

Quantum Mechanical Descriptors of Indazole-Containing Derivatives Using the DFT Method

H. Essassaoui [a], M. El idrissi [a, *], R. Bouhdadi [a], M. Echajia [a], A. Zeroual [b], A. Tounsi [a], M. Mbarki [a]

[a] Sultan Moulay Slimane University, Morocco
[b] Chouaïb Doukkali University, El Jadida, Morocco

Abstract

Indazole-containing derivatives represent one of the most important heterocycles in drug molecules. Diversely substituted indazole derivatives bear a variety of functional groups and display versatile biological activities; hence, they have gained considerable attention in the field of medicinal chemistry. In this paper, 1H-Indazole and 2H- indazole are optimized by B3LYP/6-311G (d,p) level of theory and ionization potential (IP), electron affinity (EA), and other MDs are determined. Further, non-linear optical (NLO) descriptors such as dipole moment (DM) and polarizability (α) are also determined.

Keywords: Indazole, DFT, NLO, electron affinity, ionization potential, dipole moment, polarizability and thermodynamic properties.

1. Introduction

The nitrogen-containing heterocycles are important building blocks for many bioactive natural products and commercially available drugs. As pharmacologically important scaffolds, they have attracted considerable attention from chemists (Gao, et al., 2016). Indazoles are one of the most important classes of nitrogen-containing heterocyclic compounds bearing a bicyclic ring structure made up of a pyrazole ring and a benzene ring. Indazole usually contains two tautomeric forms: 1H-indazole and 2H- indazole (Figure 1). Since 1H-indazole is more thermodynamically stable than 2H-indazole, it is the predominant tautomer (Teixeira, et al., 2006).

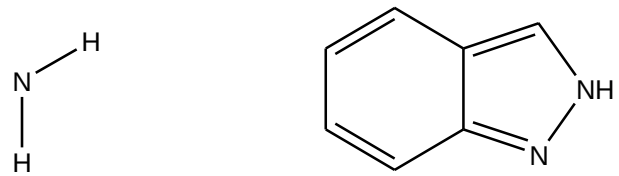

1H-Indazole **2H- indazole**

Fig. 1. Indazole nucleus

Indazole derivatives scarcely occur in nature but this particular nucleus in a variety of synthetic compounds possesses a wide range of pharmacological activities, such as anti-

* Corresponding author
E-mail addresses: idrissi_82@hotmail.fr (M. El idrissi)

inflammatory, antiarrhythmic, antitumor, antifungal, antibacterial, and anti-HIV activities (Vidyacharan et al., 2016; Shinde et al., 2016; Behrouz et al.,2017; Jayanthi et al.,2017; Popowycz et al., 2018; Bogonda et al., 2018).

Diversely substituted indazole-containing compounds furnished with different functional groups represent significant pharmacological activities and serve as structural motifs in drug molecules. For example, Bendazac and Benzydamine are two commercially available anti-inflammatory drugs that contain the 1H-indazole scaffold (Figure 2) (AI-Bogami et al., 2016).

There are some excellent reviews that have been published on the biological properties of this class of compounds (Chapolikar et al., 2015; Wang et al., 2018; Tang et al., 2018). This review serves as a comprehensive overview of recent literature that references the synthesis and biological activities of novel indazole-containing derivatives.

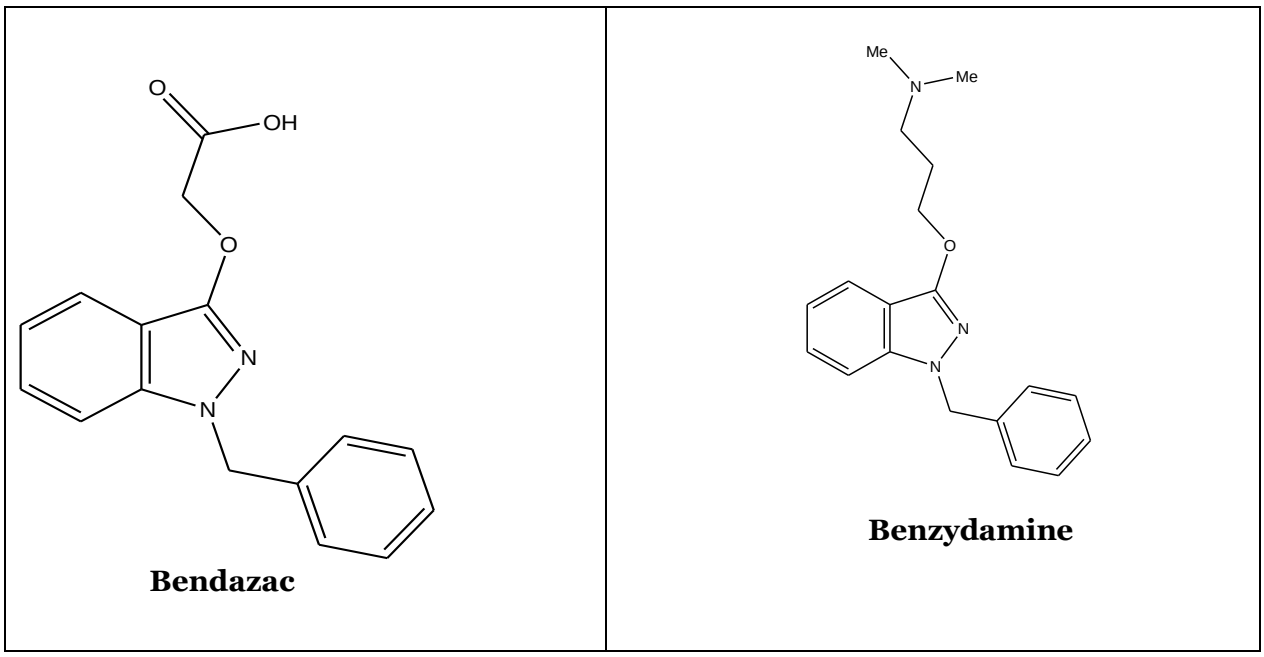

Fig. 2. Chemical structure of indazole-containing drugs

2. Computational methods

Gaussian 09 revision-B. 01-SMP (Wang et al., 2018) and Gauss View 5.0.9 (Chapolikar et al., 2015; Tang et al., 2018) are used as Earlier (Bandyopadhyay et al., 2017) for all computations. Structures were drawn in GAUSS VIEW 5.0.9 [11] of GAUSSIAN (Wang et al., 2018) software package. Initial structures were cleaned repeatedly to obtain normalized geometry. Each of the P1 and P2 was then subjected for successive optimization using semi-empirical (PM3), Hartree–Fock, and DFT methods in conjunction with appropriate basis sets. Final optimization of these molecules is achieved using DFT/B3LYP/6-311G (d, p) method. For computation of linear and NLO properties, the additional key of "optical" was included in the study. Following equations are used for the extraction of parameters and properties of these products. HOMO and LUMO energies are directly extracted from the LOG file of the corresponding optimized structure. The following formula is then used to obtain other dependent QM parameters. *IP* is the amount of energy required to take away one electron from a neutral molecule (*M*) and *EA*, oppositely, is the amount of energy released when an electron is added to a *Molecule*.

$$\mathbf{M + I} \longrightarrow \mathbf{M^+ + e}$$

Thus, $I = E(M^+) - E(M)$

$$\mathbf{M + e} \longrightarrow \mathbf{M^- + A}$$

Thus, $A = E(M) - E(M^-)$

μ is the ability of a molecule to participate in the chemical reaction. It can either be positive or negative. It is one of the very important parameters for the determination of the reactivity nature of a molecule. It is referred to as negative of electronegativity (χ) which is estimated as:

$$\mu = -\left(\frac{\delta E}{\delta N}\right)_V = -\left(\frac{\delta E}{\delta \rho}\right)_V = -\left(\frac{I+A}{2}\right);\ \ \chi = \left(\frac{I+A}{2}\right)$$

η is a very important parameter that allows understanding of the chemical reactivity of a molecule. It is the slope of the curve of μ, in electronic energy (E) versus electron number plot. In other words, η is the curvature of the μ curve. The value is always positive. However, lower the value, the higher the reactivity of the molecule. η and its reciprocal (i.e., σ) are computed as:

$$\eta = \frac{1}{2}\left(\frac{\delta c}{\delta N}\right)_V = \frac{1}{2}\left(\frac{\delta^2 E}{\delta N^2}\right) = \left(\frac{I-A}{2}\right);\ \sigma = \frac{1}{\eta}$$

Global electrophilicity index (ω) has been worked out [8] using the μ and η parameters.

$$\omega = \frac{\mu^2}{2\eta}$$

While dipole moment (*DM)* is the measure of α of a molecule in its ground state, α is the intrinsic capacity of a molecule of having a dipole when it is assaulted with an external electric field. If a molecule is present in a weak, static electric field (of strength, *F*), then the total energy (*E*) of the molecule can be express as a Taylors series.

$$E_F = E_0 - \mu_\alpha F_\alpha - \frac{1}{2!}\alpha_{\alpha\beta}F_\alpha F_\beta - \frac{1}{3!}\alpha_{\alpha\beta\gamma}F_\alpha F_\beta F_\gamma - \frac{1}{4!}\alpha_{\alpha\beta\gamma\delta}F_\alpha F_\beta F_\gamma F_\delta - \ldots$$

E_O denotes the energy of the molecule in the absence of an external electrical field. Energy ($\boldsymbol{E_o}$), dipole moment ($\boldsymbol{\mu\alpha}$), polarizability ($\boldsymbol{\alpha_{\alpha\beta}}$), and first- and second-order hyperpolarizability ($\boldsymbol{\beta_{\alpha\beta\gamma}}$ and $\boldsymbol{\gamma_{\alpha\beta\gamma\delta}}$, respectively) denote the molecular properties. First polarizability and second hyperpolarizabilities are expressed as tensor quantities, whereas subscripts single, double, etc., denote the first-rank and second-rank tensor, etc., in Cartesian coordinate.

If the external field lies on any one of the three orthogonal Cartesian axes, then the components of the induced moments will be parallel to the field. In that case, off-diagonal terms of the tensor, $\boldsymbol{\alpha_{\alpha\beta}}$ vanish. Under this conditions, the expected value of α and DM obtained as:

$$\mathrm{DM} = \sqrt{\left(\mu_X^2 + \mu_Y^2 + \mu_Z^2\right)}$$

$$\text{Or}\quad \langle \alpha_{STATIC} \rangle = \frac{\left(\alpha_{XX} + \alpha_{YY} + \alpha_{ZZ}\right)}{3}$$

In case of the anisotropic orientation of the external field, the anisotropy of the polarizability (<$\Delta\alpha$>) can be computed as:

$$\langle \Delta\alpha \rangle = \left[\frac{\left(\alpha_{XX} - \alpha_{YY}\right)^2 + \left(\alpha_{YY} - \alpha_{ZZ}\right)^2 + \left(\alpha_{YY} - \alpha_{ZZ}\right)^2 + 6\left(\alpha_{XY}^2 + \alpha_{XY}^2 + \alpha_{YZ}^2\right)}{2}\right]^{\frac{1}{2}}$$

Similarly, the first-order ($\boldsymbol{\beta_{\alpha\beta\gamma}}$) and second-order ($\boldsymbol{\gamma_{\alpha\beta\gamma\delta}}$) hyperpolarizability is calculated from components of respective tensors that are obtained from the GAUSSIAN output file.

$$\langle \beta_{STATIC} \rangle = \left[\beta_X^2 + \beta_Y^2 + \beta_Z^2\right]^{\frac{1}{2}}$$

$$\beta_i = \beta_{iii} + \frac{1}{3}\sum_{i \neq k}\left(\beta_{ikk} + \beta_{kik} + \beta_{kki}\right)$$

$$\langle \beta_{STATIC} \rangle = \left[\left(\beta_{XXX} + \beta_{XYY} + \beta_{XZZ}\right)^2 + \left(\beta_{YYY} + \beta_{YZZ} + \beta_{YXX}\right)^2 + \left(\beta_{ZZZ} + \beta_{ZXX} + \beta_{ZYY}\right)^2\right]^{\frac{1}{2}}$$

$$\langle \gamma_{STATIC} \rangle = \frac{\gamma_{XXXX} + \gamma_{YYYY} + \gamma_{ZZZZ} + 2\gamma_{YYXX} + 2\gamma_{YYZZ} + 2\gamma_{ZZXX}}{5}$$

All these optical terms have been calculated using appropriate basis set that contains polarized and diffused functions for high accuracy, in that DFT/B3LYP/6-311G(d,p) was preferred.

3. Results and discussion

3.1. Bond length and angle properties

Quantum mechanically optimized structures are shown in Figure 2. The seared used to determine selective bond lengths (in Å) and angles (in degree), the result of which are presented in Tables 1 and 2, respectively, along with available experimental results for comparison purposes. Common atoms in the structures of these products are identified using an arbitrary numbering scheme (Figure 1). Bendazac (P1) and Benzydamine (P2). Following points are noteworthy from these tables.

First, common bond lengths are almost identical (Table 1) for these impurities (P1 and P2), that show variations (underlined: Table 1) when compared with that of itself (Table 1). Notable, due to lack of P1 and P2, last four bond lengths are not available for comparison purpose. Second, similar to bond lengths, relevant angles are also compared in Table 2. It is seen that product shows slight variations in few of its representative angles when compared with that of the impurities. However, these impurities show remarkable similarities in angles when compared among themselves.

Table 1. Bond lengths (in Å) of Bendazac and Benzydamine. *(*The experimental values of the former are extracted from the crystal structure (Johnston et al., 1998)).

Bond length in Å	Bendazac	Exp(Crystal)	Benzydamine	Exp(Crystal)
C-C	1.380	1.369	1.445	1.435
C-N	1.457	1.413	1.470	1.458
C-O	1.430	1.398	1.430	1.412
C=C	1.445	1.457	1.404	1.466
N-N	1.407	1.395	1.407	1.423
O-H	1.430	1.496	1.431	1.511

Table 2. Angles (in Å) of Bendazac and Benzydamine . *(The experimental values of the former are extracted from the crystal structure* (Johnston et al., 1998)*).*

Angles in Å	Bendazac	Exp(Crystal)	Benzydamine	Exp(Crystal)
C-C-C	109.469	109.587	109.471	109.589
C-O-H	109.502	109.688	109.607	109.654
C-N-N	159.017	160.021	109.572	109.687
C-N-C	109.487	109.657	109.471	109.566
O=C-O	109.471	109.568	109.459	109.756
C=C-C	118.452	119.112	121.138	120.987
H-C-H	109.471	109.789	109.471	110.012
C=C-H	120.270	121.021	119.111	120.231

3.2. Optimized structure, electronic parameters and properties

The highest occupied molecular orbital (HOMO) and lowest unoccupied molecular orbital (LUMO) for Bendazac (P1) and Benzydamine (P2) are presented in Figure 1, along with their optimized structures. While HOMO delocalizes over bonds of P1, and P2, it is less prominent for P1 and P2. Notably, the delocalization is uniform in P1. By the use of DFT/B3LYP/6- 311G (d, p) level of theory, the extracted energies for HOMO, LUMO, and ΔE for P1 and P2 are presented in Table 3.

Table 3. HOMO, LUMO, and band gap energies for P1 and P2 (HOMO and LUMO are directly extracted from the LOG file of the Gaussian optimized structure. The band gap is computed by $E_{LUMO} - E_{HOMO}$)

Molecule	HOMO (eV)	LUMO (eV)	Band gap (eV)
Bendazac	-6.004	-3.305	2.698
Benzydamine	-3.431	-0.581	2.849

We have computed adiabatic **IP** and adiabatic **EA** for P1 and P2 and presented in Table 4.Value deviates from the mean value are highlighted by underline. **IP**: Ionization potential, **EA**: Electron affinity, **μ**: Chemical potential, **χ** : Electronegativity, **η** : Chemical hardness, **σ** : Chemical softness (**1/η**), **ω** : Electrophilicity index.

*Mean of IP and EA is 7.5 eV and 0.4 eV, respectively (Schipper et al., 2000).

Table 4. Computation of electron affinity, ionization energy, chemical potential, electronegativity, chemical hardness, chemical softness, and electrophilicity index for P1 and P2 products

All Molecule units are in (eV)							
Molecule	**IP**	**EA**	**M**	**X**	**η**	**σ**	**ω**
P1	6.004	3.305	-4.654	4.654	2.699	0.370	4.012
P2	3.431	0.581	-2.006	2.006	2.849	0.351	0.706

The highest occupied molecular orbital (HOMO) and lowest unoccupied molecular orbital (LUMO) for P1 and P2 are presented in Figure 3, along with their optimized structures, While HOMO delocalizes over bonds of P1 and P2, it is less prominent of P1 and P2. Notably, the delocalization is uniform in P1. In turn, the LUMO is mostly located for P1 and P2. By the use of DFT/B3LYP/6- 311G (d,p) level of theory.

Molecules	HOMO Energy	LUMO Energy
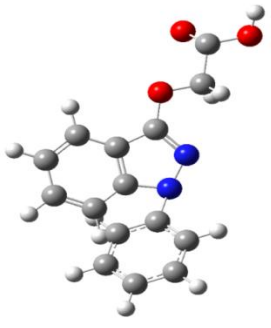 ***P1***	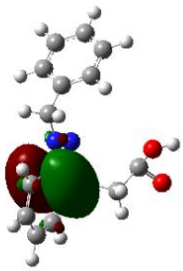	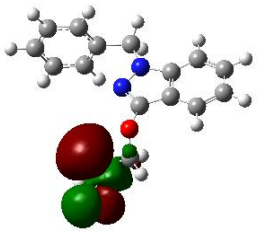

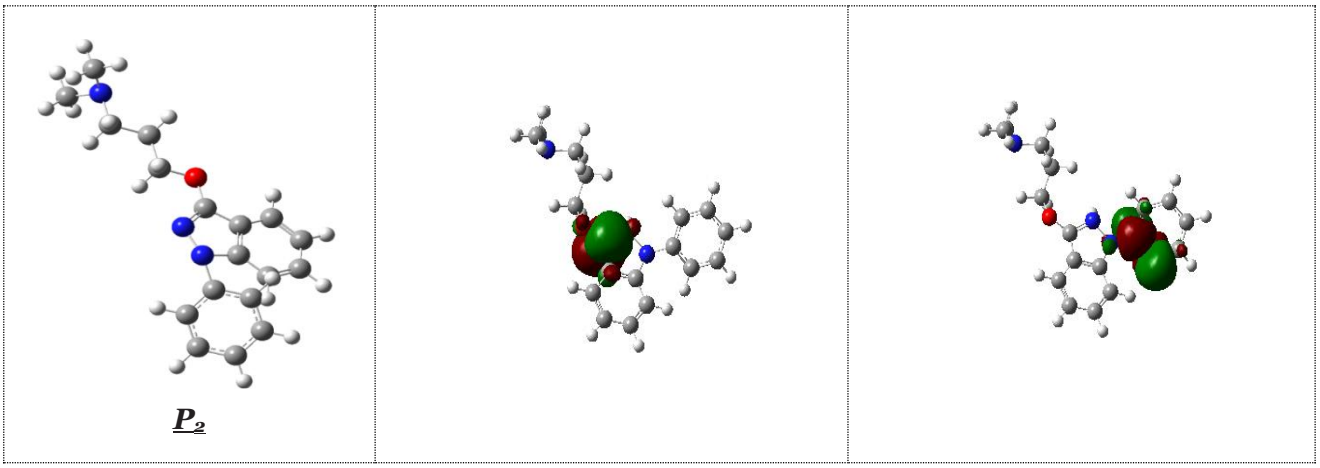

Fig. 3. Energy optimized structures (left column) along with highest occupied molecular orbitals (middle panel) and lowest unoccupied molecular orbitals (right panel) or frontier molecular orbitals of P1 and P2

The Table 4 shows that IP of P1 is higher than IP of P2. Here, P1 is seen to be anomalously high and P2 almost similaras the mean value of normal drugs (Bogonda et al., 2018). High *IP* implies low tendency for the formation of the cation. On the other hand, higher the *EA*, greater is the tendency for the formation of an anion. Although, the mean value of EA for normal drugsis ~0.6 eV, the posses shigh P2 and low (for P1) values of *E*A, μ, χ, η, σ, and electrophilicity index (ω) properties are also presented in Table 4. All these properties are dependable on *IP* and *EA*. It is seen that ω value follows the similar order as EA, P1>P2.

3.3. Non-linear optical (NLO) of P1 and P2

Intermolecular interactions such as drug-protein/DNA/RNA arelargely understood by DM, α, and first-order and second-order hyperpolarizability energy terms (Hurst et al., 1998), which are reliably computed by RB3LYP/6-311G (d,p) level of the theory (Bandyopadhyay et al., 2017). How are these parameters affected for P1 and P2. To check this above basis set is used and dipole moments (DM), α, and first- and second-rank hyperpolarizability are determined. Isotropic *DM* is presented in Table 5.

Table 5. Cartesian components and net electric dipole moments (*DM* in Debye) for P1 and P2

Names	DM_X	DM_Y	DM_Z	DM_{Total}
P_1	0.965	-3.257	-2.437	4.181
P_2	2.439	-1.665	-1.412	3.274

It is seen that the X and Y components are zero in all the cases with the Z component constituting the total *DM*. Higher and lower DM_{TOTAL} than the reported mean value are highlighted by the Table 6. Here, P1 and P2 show higher and lower DM_{TOTAL}, respectively.

Molecular complexity is the criterion that can be related with Δα (Chen et al., 2017; Aihara et al., 1999; Obot et al., 2009; Ghanadzadeh et al., 2000; Zhan et al., 2003; Xue et al., 2004; Xue et al., 1999; Lim et al., 1999; Hansch et al., 2003; Boger et al., 2003; Lee et al., 2001). More the complexity of structure more is the anisotropy of polarizability (Δα).

*Higher and lower values are underlined with respect to the mean of α, which is 34×10^{-24} esu (Schipper, et al., 2000).

Table 6. Components and mean isotropic (α) and anisotropic ($\Delta\alpha$) polarizability (in 10^{-24} esu unit) for P1 and P2

Name	α_{xx}	α_{yx}	α_{yy}	α_{zx}	α_{zy}	α_{zz}	α	$\Delta\alpha$
P_1	18.734	-4.053	21.054	-7.503	-3.174	27.253	12.343	17.506
P_2	22.175	2.214	18.467	-5.719	3.468	21.287	20.646	12.628

α, its components, and anisotropic terms are shown in Table 6. The α of P1 is seen to be much lower than α in P2 case. In these aspects, P2 is seen to be less affected (Table 6). Similar is the case for the anisotropy of polarizability ($\Delta\alpha$) and diagonal components of polarizability (α_{XX}, α_{YY}, and α_{ZZ}), where P1 have much lower value than P2. Is there any relation of α with chemical reactivity.

If molecular hardness and softness are compared with the α profile (Table 4), we see that it is inversely and directly relation with the α (Table 6), respectively. Which of the three P1 is most polarizable and which one is most active chemically.

It is seen that P1 is mor polarizable than P2. It is also seen that it possesses lowest hardness and highest softness. Interestingly, the anisotropy of α of P2 is also higher than P1.

3.4. Molecular electrostatic potential and reactivity for title compounds

The electron density is considered a very important factor for understanding the reactivity of electrophilic and nucleophilic sites and the interactions of hydrogen bonding (Gresh et al., 2007; Scrocco et al., 1979; Luque et al., 2000), as well as this density, is related to the molecular electrostatic potential (MEP). Therefore for predicting this reactivity of nucleophilic and electrophilic sites attacks for studied compounds, we simulated the MEP of these compounds using the B3LYP level of the optimized geometry. The different colors (red, blue and green) at the MEP surface represent different values of the electrostatic potential as the regions of most negative, most positive and zero electrostatic potential respectively. The negative electrostatic potential at the MEP (shades of red) indicates that this region is attractive of the proton by the aggregate electron density in the molecule, while the positive electrostatic potential (shade of blue) is the region that presents of the repulsion of the proton by the atomic nuclei. The negative regions at MEP (red) correspond to electrophilic reactivity (regions of most electronegative electrostatic potential) and the positive region(blue) correspond to nucleophilic reactivity (regions of the most positive electrostatic potential) and green represent regions of zero potential.

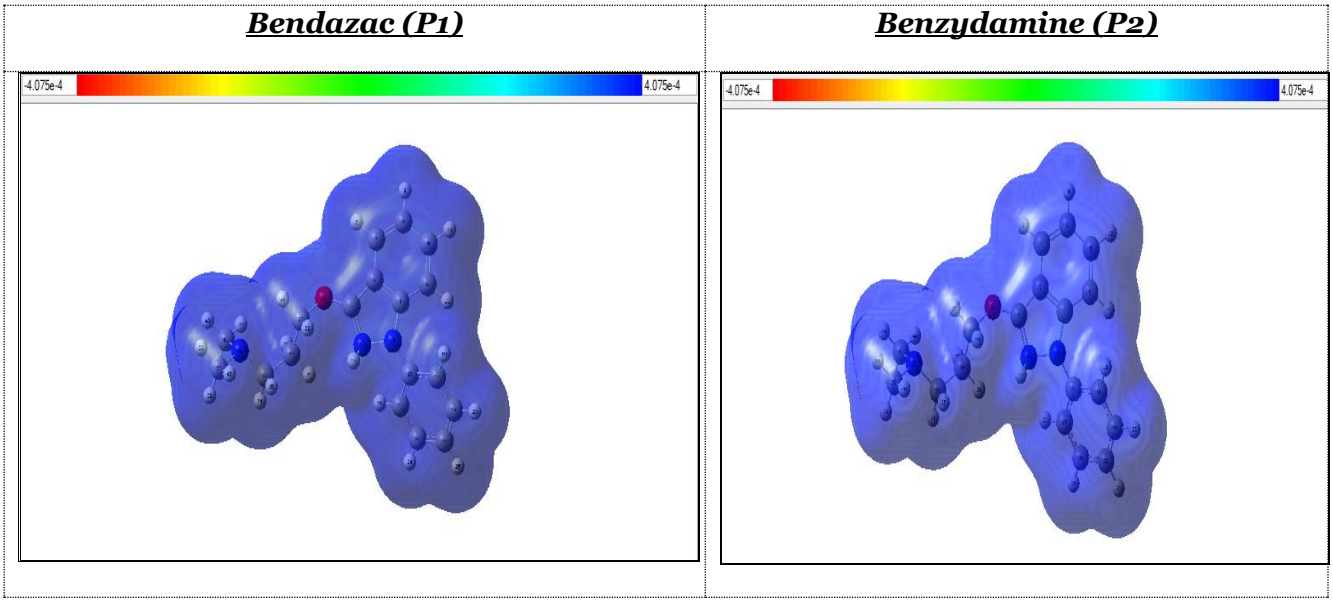

Fig. 4. Calculated electrostatic potential surfaces on the molecular surfaces of studied compounds P1 and P2. (Color ranges, in kcal/mol: from red –4.075 10^{-4} to blue +4.075 10^{-4} B3LYP functional and 6-311G (d,p) basis set)

3.3. Thermodynamic properties

Computation of thermodynamic properties of P1 and P2 products is important for both thermochemistry and chemical equilibrium. Statistical thermodynamics with the two keyideas, Boltzmann distribution and the partition function leads to the derivation of the equations utilized for computing thermochemical enthalpy (ΔH^o), dipole moment and the rotational constants of the molecular system were obtained directly from the output of Gaussian calculation employing B3LYP/6-311G(d.p) basis set and are listed in the Tables 7a, 7b and 7c.

Table 7a. Variation of different thermodynamic parameters with temperature (Bendazac P1)

Temperature (K)	Enthalpy ΔH (Kcal/mol)	Entropy ΔS (Cal/mol.K)	Specific heat C_P (Cal/mol.K)
100	-588.841	159.218	34.215
200	-586.326	162.354	39.124
300	-581.023	163.897	42.147
400	-576.236	165.027	45.678
500	-571.056	169.874	49.785
600	-562.453	171.236	51.013
700	-559.367	175.965	52.698
800	-550.259	177.889	55.234

Table 7b. Variation of different thermodynamic parameters with temperature (Benzydamine P2)

Temperature (K)	Enthalpy ΔH (Kcal/mol)	Entropy ΔS (Cal/mol-K)	Specific heat C_P (Cal/mol.K)
100	-598.075	126.459	36.458
200	-596.245	130.256	39.789
300	-594.879	135.789	43.012
400	-591.023	131.671	46.358
500	-585.214	128.369	50.247
600	-581.789	123.458	53.697
700	-575.984	120.444	55.489
800	-570.325	117.885	59.782

Table 7c. Different thermodynamic parameters at room temperature (P1 and P2)

	B3LYP/6-311G (d,p)	
Parameters	**Bendazac (P1)**	**Benzydamine (P2)**
Total energy (Hartree)	-953,105	-938,389
Zero-point vibrational energy (Kcal/mol)	167,546	231,903
Rotational constants (GHz)	0,465	0,564
	0,548	0,621
	0,789	0,879

The correlation between temperature and these thermodynamic properties are given by Figure 5. The correlation equations are as follows:

$$H_m^0 = -599.3586 - 0.0389\ T - 9.2154.10^{-4}\ T^2 \quad (R^2 = 0.9145)$$
$$S_m^0 = 121.337 + 0.3547\ T - 5.3214.10^{-4}\ T^2 \quad (R^2 = 0.9575)$$
$$Cp_m^0 = 1.2574 + 0.2447\ T - 3.2248.10^{-4}\ T^2 \quad (R^2 = 0.9715)$$

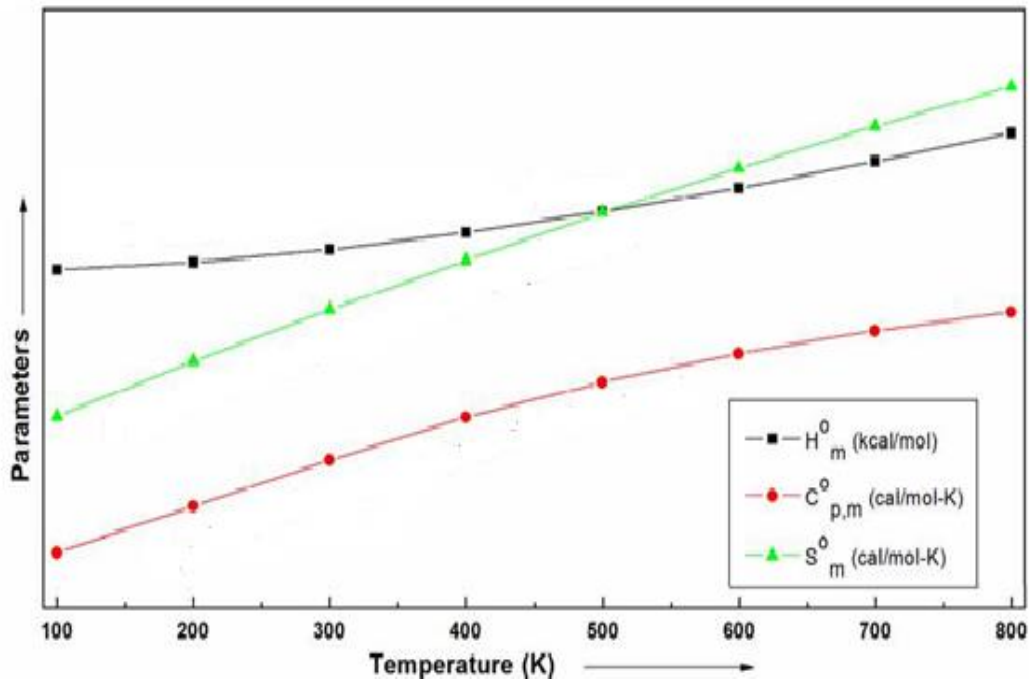

Fig. 5. Correlation between different thermodynamic properties with the temperature

It is observed that the parameters increase from 100 to 800 K due to the increase in the molecular vibrational intensities with the temperature.

4. Conclusion

Electronic structural properties for representative the P1 and P2 products are worked out by RB3LYP/6-311G (d, p) level of theory of Gaussian 09 software package. The ground state optimized structures are used for computation of electronic and NLO properties. Corresponding bond lengths and angles of these products show remarkable similarity among themselves but show variation.

The observation of high *EA*, low band gap, low η, high χ, and high *IP* of P1 may indicate that is are strongly electrophilic in nature.

P1 product more polarizable, hyperpolarizable and chemically more reactive compared to P2. So P1 it is more interactive to target molecule.

5. Conflict of Interest

The authors declare that there is no conflict of interests regarding the publication of this paper. Also, they declare that this paper or part of it has not been published elsewhere.

6. Acknowledgments

The authors are thankful for Laboratory of Chemical Process and Applied Materials. Sincere thanks are also due for Prof. Mohamed Mbarki, Department of Chemistry and Environment, Faculty of Science and Technologies. Sultan Moulay Slimane University, Moroco, for valuable comments for the manuscript.

References

AI-Bogami et al., 2016 – *AI-Bogami A.S.* (2016). Mechano chemical synthesis of cyclohexenones and indazoles as potential antimicrobial agents. *Res. Chem. Intermed.*, 42, 5457-5477.

Aihara et al., 1999 – *Aihara JI.* (1999). Reduced HOMO-LUMO gap as an index of kinetic stability for polycyclic aromatic hydrocarbons. *J Phys Chem A.,* 103: 7487-95.

Bandyopadhyay et al., 2017 – *Ansary I., Das A., Gupta P.S., Bandyopadhyay A.K.* (2017). Synthesis, molecular modeling of N-acyl benzoazetinones and their docking simulation on fungal modeled target. *Synth Commun,* 47: 1375-86.

Behrouz et al., 2017 – *Behrouz S.* (2017). Highly efficient one-pot three component synthesis of 2H-indazoles by consecutive condensation, C-N and N-N bond formations using Cu/Aminoclay/reduced grapheme oxide nanohybrid. *J. Heterocyclic. Chem.,* 54, 1863-1871.

Boger et al., 2003 – *Boger DL., Desharnais J., Capps K.* (2003). Solution-phase combinatorial libraries: Modulating cellular signaling by targeting protein-protein or protein-DNA interactions. *Angew Chem Int Ed Engl.,* 42: 4138-76.

Bogonda et al., 2018 – *Bogonda G., Kim H.Y., Oh K.* (2018). Direct acyl radical addition to 2H-indazoles using Ag-catalyzed decarboxylative cross-coupling of α-keto acids. *Org. Lett.*, 20, 2711-2715.

Chapolikar et al., 2015 – *Gaikwad DD, Chapolikar AD, Devkate CG, Warad KD, Tayade AP, Pawar RP, Domb AJ.* (2015). Synthesis of indazole motifs and their medicinal importance: Anover view. *Eur. J. Med. Chem.,* 90, 707-731.

Chen et al., 2017 – *Chen L., Lu J., Huang T., Cai YD.* (2017). A computational method for the identification of candidate drugs for non-small cell lung cancer. *PLoS One,* 12: e0183411.

Gao et al., 2016 – *Gao M., Xu, B.* (2016). Transition metal-involving synthesis and utilization of N-containing heterocycles: Exploration of nitrogen sources. *Chem. Rec.,* 16, 1701-1714.

Ghanadzadeh et al., 2000 – *Ghanadzadeh A., Ghanadzadeh H., Ghasmi G.* (2000). On the molecular structure and aggregative properties of Sudan dyes in the anisotropic host. *J Mol Liq.,* 88: 299-308.

Gresh et al., 2007 – *Cisneros GA., Darden TA., Piquemal JP.* (2007). Anisotropic, polarizable molecular mechanics studies of inter- and intramolecular interactions and ligand-macromolecule complexes. A Bottom-up strategy. *J. Chem Theory Comput.,* 3: 1960-86.

Hansch et al., 2003 – *Hansch C., Steinmetz WE, Leo AJ, Mekapati SB, Kurup A, Hoekman D.* (2003). On the role of polarizability in chemical-biological interactions. *J. Chem Inf Comput Sci.,* 43: 120-125.

Hurst et al., 1998 – *Hurst GJ., Dupuis M., Clementi E.* (1998). A binitio analytic polarizability, first and second hyperpolarizabilities of large conjugated organic molecules: Applications to polyenes C4H6 to C22H24. *J. Chem Phys.,* 89: 385-95.

Jayanthi et al., 2017 – *Jayanthi M., Rajakumar P.* (2017). Synthesis, cell viability, and flow cytometric fluorescence pulse width analysis of dendrimers with indazoles surface unit. *J. Heterocyclic. Chem.,* 54, 3042-3050.

Johnston et al., 1998 – *Harris K.D.M., Johnston R.L., Kariuki B.M.* (1998). Acta Crystallogr. Sect. A: Found. *Crystallogr,* 54: 632-645.

Lee et al., 2001 – *Lee JY, Kim KS, Mhin BJ.* (2001). Intramolecular charge transfer of π-conjugated push-pull systems in terms of polarizability and electronegativity. *J. Chem Phys.,* 115: 9484-9.

Lim et al., 1999 – *Lim I.S., Pernpointner M., Seth M., Laerdahl J.K., Schwerdtfeger P., Neogrady P.* (1999). Relativistic coupled-cluster static dipole polarizabilities of the alkali metals from Li to element 119. *Phys Rev A.,* 60: 2822.

Luque et al., 2000 – *Luque F.J., Lopez J.M., Orozco M.* (2000). Perspective on electrostatic interactions of a solute with a continuum. A direct utilization of ab initio molecular potentials for the prevision of solvent effects. *Theor. Chem. Acc.,* 103, 343-345.

Obot et al., 2009 – *Obot IB., Obi-Egbedi NO., Umoren SA.* (2009). Antifungal drugs as corrosion inhibitors for aluminium in 0.1 M HCl. *Corrosion Science*, 51(8): 1868-75.

Popowycz et al., 2018 – *Lavrard H., Popowycz F.* (2018). Regioselective late-stage C-3functionalization of pyrazolo-[3,4-b]pyridines. *Synthesis,* 50, 998-1006.

Schipper et al., 2000 – *Schipper PR, Gritsenko OV, Van Gisbergen SJ, Baerends EJ.* (2000). Molecular calculations of excitation energies and (hyper) polarizabilities with a statistical average of orbital model exchange-correlation potentials. *J. Chem Phys.,* 112: 1344-1352.

Scrocco et al., 1979 – *Scrocco E., Tomasi J.* (1979). Electronic molecular structure, reactivity and intermolecular forces: an heuristic interpretation by means of electrostatic molecular

potentials, Adv. *Quantum Chem.,* 1, 115-121.

Shinde et al., 2016 – *Shinde A., Vidyacharan H.S., Sharada D.S.* (2016). BF3-OEt2 mediated metal-free one-pot sequential multiple annulation cascade (SMAC) synthesis of complex and diverse tetrahydro isoquinoline fused hybrid molecules. *Org. Biomol. Chem.*, 14, 3207-3211.

Tang et al., 2018 – *Wan Y.C., He S.Z., Li W., Tang Z.L.* (2018). Indazole derivatives: Promising anti-tumor agents. Anti-Cancer Agents. *Med. Chem.*, 18, DOI: 10.2174/1871520618 666180510113822

Teixeira et al., 2006 – *Teixeira F.C., Ramos H., Antunes I.F., M. João M. Curto, Teresa Duarte M., Bento I.* (2006). Synthesisandstructural characterization of 1-and 2-substituted indazoles: Ester and carboxylic acid derivatives. *Molecules,* 11, 867–889.

Vidyacharan et al., 2016 – *Vidyacharan S., Murugan A., Sharada D.S.* (2016). C(sp2)-H Functionalization of 2H-indazoles at C3-position via palladium(II)-catalyzed isocyanide insertion strategy leading to diverse heterocycles. *J. Org. Chem.,* 81, 2837-2848.

Wang et al., 2018 – *Dong J.Y., Zhang Q.J., Wang Z.T., Huang G., Li S.S.* (2018). Recent advances in the development of indazole- based anticancer agents. *Chem. Med. Chem.,* 13, 1490-1507.

Xue et al., 1999 – *Harris P.G., Baker C.A., Green K., Iaydjiev P., Ivanov S.I, May D.J.* (1999). New experimental limit on the electric dipole moment of the neutron. *Phys Rev Lett.,* 82: 904.

Xue et al., 2004 – *Xue Y., Li ZR., Yap CW., Sun LZ., Chen X., Chen YZ.* (2004). Effect of molecular descriptor feature selection in support vector machine classification of pharmacokinetic and toxicological properties of chemical agents. *J Chem Inf Comput Sci.,* 44: 1630-8.

Zhan et al., 2003 – *Zhan CG, Nichols JA, Dixon DA.* (2003). Ionization potential, electron affinity, electronegativity, hardness, and electron excitation energy: Molecular properties from density functional theory orbital energies. *J. Phys Chem A.,* 107: 4184-95.